



Multiphoton excitation of CH_3I

Eiríkur Þórir Baldursson



**Faculty of Physical Sciences
University of Iceland
2012**

Multiphoton excitation of CH₃I

Eiríkur Þórir Baldursson

16 ECTS thesis as a part of
Baccalaureus Scientiarum degree in Chemistry

Supervisors:
Prof. Ágúst Kvaran

Faculty of Physical Sciences
School of Engineering and Natural Sciences
Univeristy of Iceland
Reykjavík, Mai 2012

Multiphoton ionization of CH_3I

16 ECTS thesis as a part of *Baccalaureus Scientiarum* degree in Chemistry

Copyright © 2012 Eiríkur Þórir Baldursson

All rights reserved

Faculty of Physical Sciences

School of Engineering and Natural Sciences

University of Iceland

VRII, Hjarðarhagi 2-6

107 Reykjavík

Telephone: 525 4000

Registration information:

Eiríkur Þórir Baldursson, 2012, *Multiphoton excitation of CH_3I* , BS thesis, Faculty of Physical Sciences, University of Iceland, 33 bls.

Print: Háskólaprent

Reykjavík, Mai 2012

Útdráttur

(2+n) 2D-fjölljóseindalitróf af CH_3I var skráð fyrir örvunarorkubilið $64880\text{ cm}^{-1} - 71480\text{ cm}^{-1}$. Mæligögn einstakra jóna í 2D-fjölljóseindalitrófinu voru teguð til að mynda 1D-fjölljóseindalitróf af C^+ , I^+ og CH_3^+ . Tvær fyrstnefndu jónirnar gáfu einungis skarpar atóm línur sem voru bornar saman við tilraunagildi frá NIST. CH_3^+ gaf breiða sameinda-gleypnitoppa vegna tilfærslna í Rydberg ástönd. Ásamt Rydberg ástöndunum sem sáust voru tveir titringstoppar frá CH_3^* radikalnum. Einn af þeim hafði sést fyrr.

2D-REMPI merki I^+ sást í öllum mælingum, ólíkt hinum jóna brotunum. Þetta bendir til þess að CH_3I brotnar auðveldlega niður í CH_3 og I brot. Þetta er útskýrt með niðurbrots skema CH_3I sem felur í sér tvær leiðir til myndunar I atóms.

Abstract

(2+*n*) 2-D REMPI spectra of CH₃I were recorded for the excitation energy region 64880 cm⁻¹ – 71480 cm⁻¹. Signals for individual ions were integrated to obtain 1D-REMPI spectra of C⁺, I⁺ and CH₃⁺. The first two fragments displayed only sharp atomic lines that were compared to values provided by NIST. CH₃⁺ showed broad molecular absorption peaks that were assigned to Rydberg states. Along with the Rydberg states observed, two vibrational bands due to the CH₃^{*} radical were observed, one of which could not be found in previous experiments.

I⁺ signals were observed in every measurement, unlike other ion fragments. This suggests that CH₃I readily breaks into CH₃ and I fragments. This is explained via the dissociation schematic of CH₃I which involves two pathways for forming I atoms.

Ég lýsi því hér með yfir að þessi ritgerð er samin af mér og að hún hefur hvorki að hluta né að í heild verið lögð fram áður til hærri prófagráðu.

I herby declare that this report is written by me and has not been handed in at part or in whole for a higher education degree.

Eiríkur Þórir Baldursson

Index

Figure index	viii
Table index	ix
Acronyms.....	x
Acknowledgments	xi
1 Introduction.....	1
2 Experimental Setup and Procedure	3
3 Results and Analysis	5
3.1 2D-REMPI data	5
3.2 Power dependence	7
3.3 Ion formation	9
3.4 C^+ 1D-REMPI	11
3.5 CH_3^+ 1D-REMPI / Rydberg states	14
3.6 CH_3^* vibrational bands	19
3.7 I^+ 1D-REMPI.....	21
4 Conclusions.....	24
References.....	25
Appendix	27

Figure index

Figure 2.1	The measured output power of the dyes used in this experiment along with the scan range	3
Figure 3.1	2D-REMPI: Mass spectra of CH ₃ I and the (CH ₃ I) ₂ dimer for the excitation region 69200 cm ⁻¹ – 69640 cm ⁻¹	5
Figure 3.2	2D-REMPI: Mass spectra of CH ₃ I at 20°C and with no argon backing pressure for the excitation region 69400 cm ⁻¹ – 69800 cm ⁻¹	6
Figure 3.3	A selected power dependence measurement of the I ⁺ ion signal at 17440 cm ⁻¹	7
Figure 3.4	A selected power dependence measurement of the CH ₃ ⁺ ion signal at 17646cm ⁻¹	8
Figure 3.5	A selected power dependence measurement of the CH ₃ ⁺ ion signal at 17449cm ⁻¹	8
Figure 3.6	Possible dissociation pathways of CH ₃ I. 1: Excitation to Rydberg states. 2: Curve crossing to repulsive states. 3: Fragmentaion of the CH ₃ I molecule.....	10
Figure 3.7	1D-REMPI of C ⁺ ion signal in the excitation range where it was present in the 2D-REMPI.	11
Figure 3.8	The Enlarged carbon atomic lines due to (2+n) REMPI of C(2s ² 2p ² ; ³ P ₀), C*(2s ² 2p2; ³ P ₁) and C**(2s ² 2p2; ³ P ₂).	12
Figure 3.9	A possible dissociation pathway of CH ₃ I to form C atoms and hence C ⁺ ions.....	13
Figure 3.10	Total CH ₃ ⁺ 1D-REMPI spectra, see also figs. 3.12 and 3.13.....	14
Figure 3.11	Comparison of the 1D-REMPI of I ⁺ and CH ₃ ⁺	15
Figure 3.12	a) Overall view of possible ranges for Rydberg state transitions. b)Possible ranges of Rydberg state transitions in the scan range of the 1D-REMPI for CH ₃ ⁺	16
Figure 3.13	Assigned Rydberg state transition peaks in the 1D-REMPI of CH ₃ ⁺	17
Figure 3.15	Comparison of the suspected vibrational peaks at 69848.97 cm ⁻¹ and 70626.46 cm ⁻¹	19
Figure 3.16	A sample of the trial and error fitting in estimating rotational constants.....	20
Figure 3.17	Iodine atomic lines (cm ⁻¹) due to (2+n) REMPI of I(5s ² 5p ⁵ ; ² P _{3/2}) and I*(5s ² 5p ⁵ ; ² P _{1/2}) along with previously observed transitions.	21
Figure 3.18	Suggested dissociation pathways of CH ₃ I to form I ⁺ ions. Two possible pathways are shown: The dissociation from Rydberg state transitions and the dissociation from ion pair formations.	22

Table index

Table 3.1	Transmittance of the power reducing windows used in the power dependence measurements.....	7
Table 3.2	Bond energies of the single bonds in methyl iodine.....	9
Table 3.3	Ion formation energies calculated using equation 3.2.	10
Table 3.4	Carbon atomic lines (cm^{-1}) due to (2+n) REMPI of $\text{C}(2s^22p^2; ^3P_0)$, $\text{C}^*(2s^22p^2; ^3P_1)$ and $\text{C}^{**}(2s^22p^2; ^3P_2)$	11
Table 3.5	Calculated quantum defects using previous measurements of methyl iodine and iodine transitions along with assumed defects using individual measurements of previous measurements.	15
Table 3.6	Experimental CH_3^+ peak positions compared with previously observed peaks.	17
Table 3.7	Fit parameters for vibrational bands at 69848.97 cm^{-1} and $70626.462 \text{ cm}^{-1}$	20
Table 3.8	Iodine atomic lines (cm^{-1}) due to (2+n) REMPI of $\text{I}(5s^25p^5; ^2P_{3/2})$ and $\text{I}^*(5s^25p^5; ^2P_{1/2})$	23

Acronyms

AMU:	Atomic Mass Unit
TOF:	Time Of Flight
NIST:	National Institute of Standards and Technology
REMPI:	Resonance Enhanced Multi-Photon Ionization
BBO:	Beta barium borate
UV:	Ultra-Violet
IE:	Ionization Energy

Acknowledgments

This research could not have been performed without the invaluable guidance and support of Professor Ágúst Kvaran, Victor Huasheng Wang and Jingming Long.

1 Introduction

Since they were linked to the degradation of the ozone layer, spectroscopy and photofragmentation of organic molecules containing halogens have been a subject of interest. Most studies have been focused on freons, which are organic chemical compounds containing carbon, halogens and fluorine and are derivatives of methane or ethane. The halo-organic compounds, especially freons, are very effective in ozone degradation.¹ When the halo-organic compounds are bombarded with ultra-violet radiation from the sun they form halogen radicals. The radicals attack ozone molecules which causes the formation of oxygen. This can lead to increased UV radiation on the Earth's surface which is harmful to life. This research focuses on methyl iodine, which is a halo-organic molecule. It was recently approved for use as a pesticide by the EPA and needs to be studied since chemists are skeptical about its safety.²

The study uses Resonance Enhanced Multi-Photon Ionization (REMPI) to measure excited states. The method involves using one or more photons to excite a molecule to an electronically excited state from which the molecule either dissociates or remains intact and the fragments are then ionized with additional photons. The nomenclature, $(m+n)$ REMPI, is used to describe how many photons are absorbed by the chemical of interest. The variable m describes the number of photons needed to perform resonance excitation of the molecule and the variable n describes the number of photons required to ionize the molecule or its fragments after excitation. $(2+n)$ REMPI is being observed in this research. Two photons are required to perform resonance excitation of the CH_3I molecule and an unknown number, n , of photons are used to ionize depending on the dissociation pathway of the excited molecule. Compared to the one-photon absorption, the two-photon absorption measurements result in different excitations. The selection rule depending on the orbital angular momentum quantum number, l , varies with the number of photons needed to excite the chemical. Thus different excitations are observed with REMPI.³

The Rydberg states of atoms and compounds are thermodynamically excited states which are primarily composed of atomic orbitals with principal quantum numbers, n , greater than the ground state and the valence excited states. The excitation energies follow the Rydberg formula (see eq. 1.1), where E is the transition energy, IE the ionization energy, R_H the Rydberg constant, n the principal quantum number and δ is the quantum defect.

¹ Environmental Chemistry – 4th edition. Baird, C.; Cann, N. 2008, W. H. Freeman and Company

² California under fire for approving controversial pesticide. Rebecca Trager. 2011 Royal Society of Chemistry.

³ Multiphoton Spectroscopy, Applications. Michael NR Ashfold, Colin M Western. 1999 Elsevier Ltd., Vol. 2, P. 1424.

(1.1)

$$E = IE - \frac{R_H}{(n - \delta)^2}$$

The focus of this study was on using REMPI to measure and study photodissociation of methyl iodine, CH₃I, for the excitation range of 64880 cm⁻¹ - 71480 cm⁻¹. Absorption energies were used to help estimate the photodissociation of CH₃I.

2 Experimental Setup and Procedure

Measurements were done using a tunable excitation radiation generated by Excimer laser-pumped dye laser system. The beam originated from a Lambda Physik COMPex 205 Excimer laser and passed through a Coherent ScanMatePro dye laser at a typical repetition rate of 10 Hz. Dyes C540, R590 and R610 were used for the excitation wavelengths. Frequency doubling was attained by passing the beam through a BBO crystal in a Sirah Second Harmonic Generator. The scan range and output power curves of each dye are shown in figure 2.1.

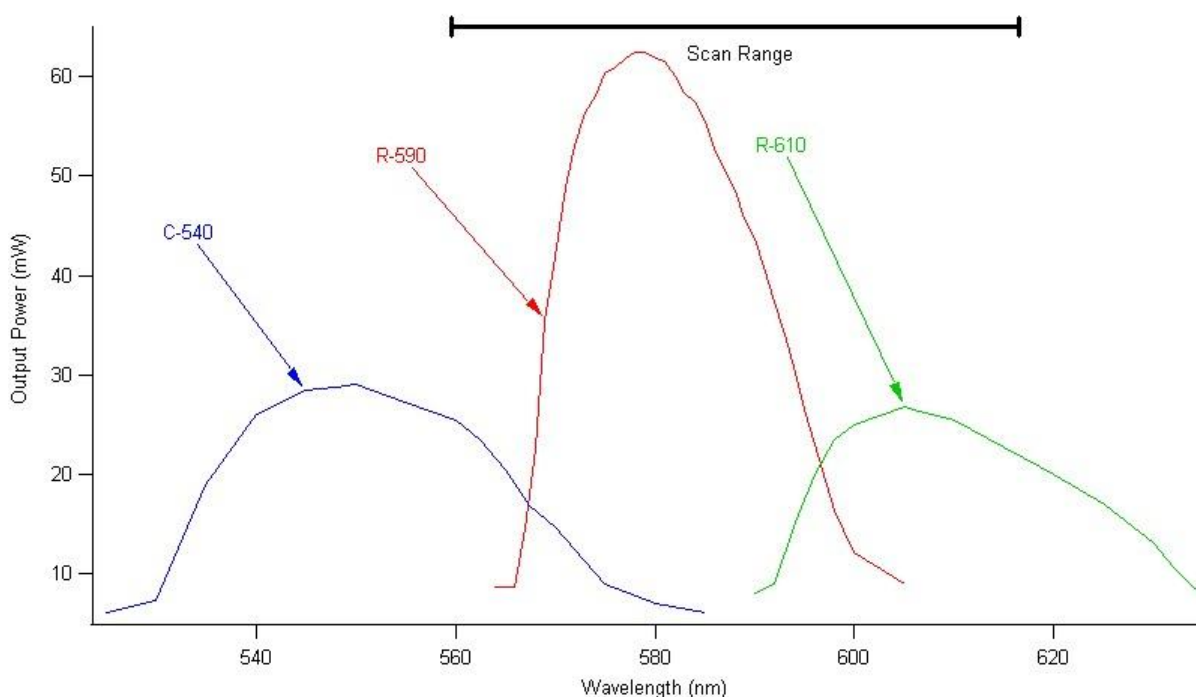


Figure 2.1; The measured output power of the dyes used in this experiment along with the scan range.

The apparatus has been described before and used in other similar experiments.⁴ Two dimensional REMPI data were recorded for a CH_3I molecular beam, created by jet expansion of a pure sample through a 500 μm pulse nozzle into a vacuated ionization chamber with a pressure of about 5×10^{-6} mbar. Ions formed by multiphoton excitation were directed into a TOF tube and detected by a micro-channel plate detector. Signals were fed into a LeCroy Wavesurfer 44MXs-A, 400MHz storage oscilloscope and stored as a function of ion time of flights and laser radiation wavenumbers (i.e. 2D-REMPI).

⁴ Photofragmentations, State Interactions and Energetics of Rydberg and Ion-pair states: Two Dimensional Resonance Enhanced Multiphoton Ionization of HBr via singlet-, triplet-, $\Omega=0$ and 2 states, Jingming Long, Helgi Rafn Hróðmarsson, Huasheng Wang, Ágúst Kvaran. 2012.

Liquid CH₃I sample was placed in a glass container immersed in an isotherm container and connected to the ionization chamber. First measurements were done with the sample container placed in a CCl₄ and liquid nitrogen cooling bath that had a temperature of about -23°C which resulted in a vapor pressure of about 40 Torr from the CH₃I sample. The sample vapor was pumped through the nozzle into the ionization chamber with a 1 bar argon background pressure. These conditions caused the appearance of a I₂⁺ peak (fig. 3.1) in the 2D-REMPI which was caused by (CH₃I)₂ dimers. Formation of the dimers was due to the cooling of the sample as well as the jet cooling when the sample expanded through the nozzle into the ionization chamber, methyl iodine dimers readily form in cool conditions.⁵ Measurements were done to find the conditions where the dimer was at minimum using different temperatures and argon backing pressure. Optimal conditions were for the sample at 20°C temperature, which lead to about 400 Torr vapor pressure of the liquid CH₃I, and no background argon pressure to reduce jet cooling of the sample while going into the ionization chamber.

The laser scan range, shown in figure 2.1, is from 616.52 nm to 559.60 nm. With the frequency doubling that corresponds to an excitation range of 64880 cm⁻¹ to 71480 cm⁻¹. Notably the scan range does not reach the maximum measured output power for C-540. This is due to low quality measurements with this dye where broad overlapping peaks appeared in the 2D-REMPI and made the data unreliable, effects of which are shown in chapter 3.5.

Power dependence of the ion signals was determined by averaging the signal for 500 pulses for a certain power. Six different quartz windows were used to reduce the laser power by decreasing the laser transmittance. For certain laser excitation energies and frequencies the ion signal areas were measured as a function of power.

All 1D-REMPI spectra were corrected for power using an energy correction procedure to be found in the appendix (page 29) in IGOR. Laser power was recorded during each scan to make this correction possible.

⁵ Effect of Dimers on the Temperature-Dependent Absorption Cross Section of Methyl Iodide, Gabriela C. G. Waschewsky, Robert Horansky, and Veronica Vaida. 1996, Journal of Physical Chemistry, Vol. 100, No. 28, P. 11559.

3 Results and Analysis

3.1 2D-REMPI data

The mass spectra obtained by the REMPI measurements were time dependent and needed to be converted into mass. This conversion is relatively easy based relationship between the time-of-flight of an ion in the TOF-tube and its mass shown in equation 3.1.

$$(3.1) \\ t_{TOF} \propto \sqrt{M_w}$$

The procedure used can be found in the appendix (page 27). The mass spectra were all very clear and identification of the individual peaks was relatively easy.

The first measurements done with cooling to $-23\text{ }^{\circ}\text{C}$ displayed a mass peak at around 254 amu which was identified as a I_2^+ signal (figure 3.1). This meant that cooling of the sample, both in the sample container and by the jet cooling when the sample entered the ionization chamber had resulted in a $(\text{CH}_3\text{I})_2$ dimer formation.

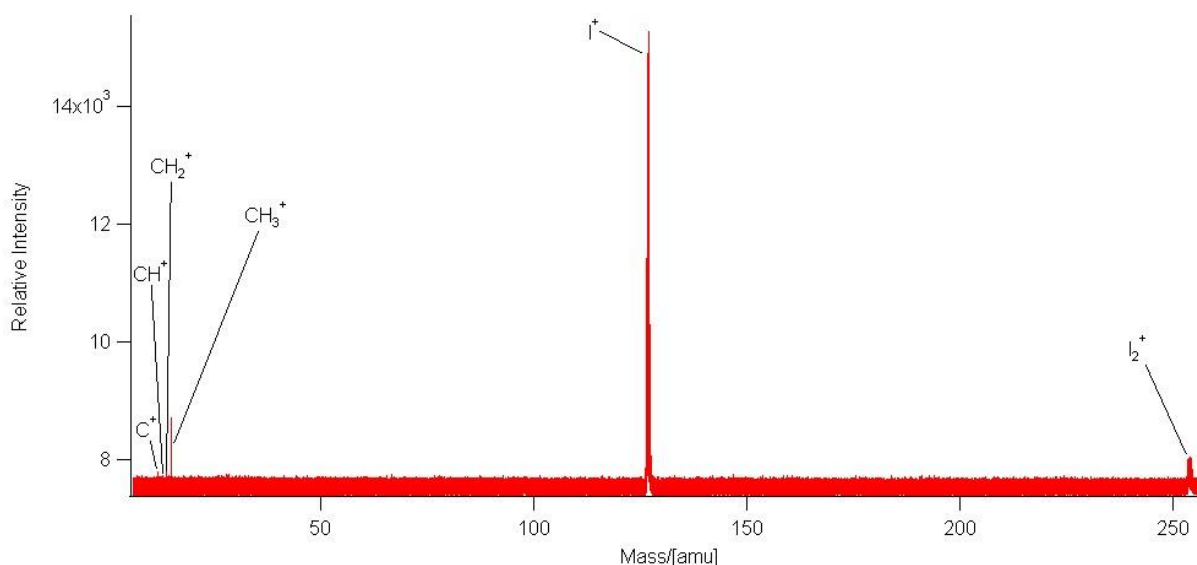


Figure 3.1; 2D-REMPI: Mass spectra of CH_3I and the $(\text{CH}_3\text{I})_2$ dimer for the excitation region $69200\text{ cm}^{-1} - 69640\text{ cm}^{-1}$.

To reduce this effect the sample temperature was increased to reduce the formation of dimers in the sample tube and the argon backing pressure was removed to reduce jet cooling of the sample upon entering the ionization chamber. This proved useful and the I_2^+ signal could not be observed. The broad appearance of the I^+ signal in figure 3.2 is caused by strong atomic lines in the I^+ signal. This became problematic to longer wavenumbers

than 70840 cm^{-1} , where the appearance of many strong lines in a short range caused overlapping of signals, even CH_3^+ 1D-REMPI displayed I^+ atomic lines.

As seen in figure 3.2 the CH_3^+ and the I^+ signals were the strongest and appeared in almost all mass spectra. The C^+ signal was present in many mass spectra but not all. CH^+ and CH_2^+ signals rarely appeared and therefore their 1D-REMPI spectra were too incomplete to use.

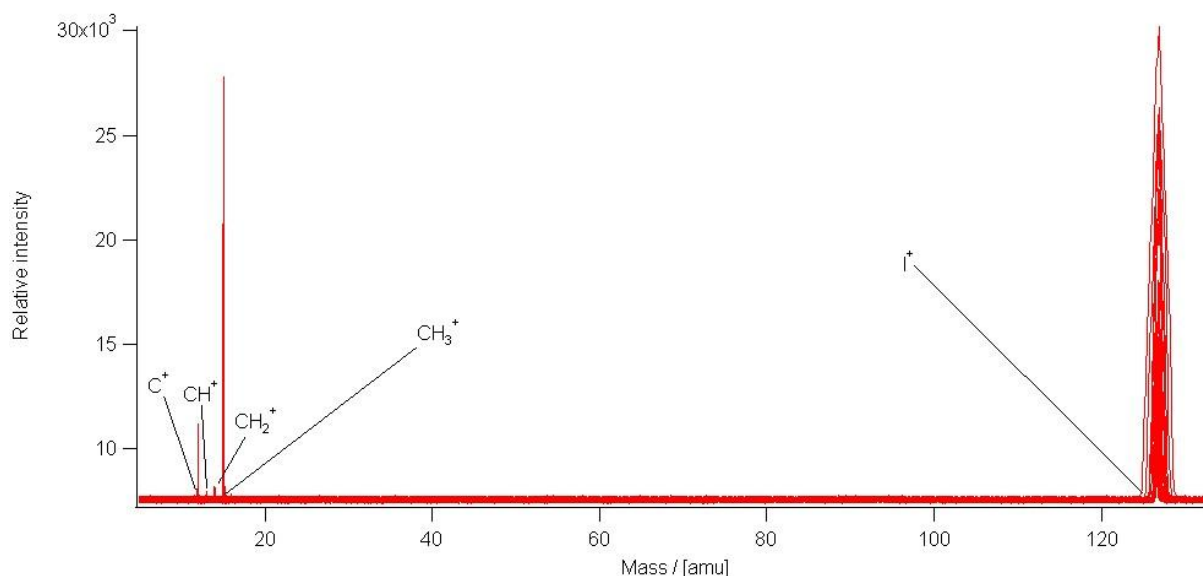


Figure 3.2; 2D-REMPI: Mass spectra of CH_3I at 20°C and with no argon backing pressure for the excitation region $69400\text{ cm}^{-1} - 69800\text{ cm}^{-1}$.

3.2 Power dependence

Power dependence was measured for the CH_3^+ and I^+ ion signals, averaging over 500 pulses for a certain power. Measurements were done using 6 different quartz windows that had varied transmittance so they would reduce the power of the laser systematically. Their effect on transmittance can be seen in table 3.1. The ion signal was integrated and the logarithm of both the relative power and relative intensity was plotted against each other. A straight line was fitted to the graph to find the slope. The slope represents the number of photons required to ionize.

Table 3.1; Transmittance of the power reducing windows used in the power dependence measurements.

Window number	% Transmittance
1	91.201%
2	90.272%
3	91.278%
4	86.704%
5	68.011%
6	82.499%

The measurements for the I^+ ion signal were done at 17440 cm^{-1} , a atomic line, and the measurements the CH_3^+ ion signal were done at 17646 cm^{-1} and 17449 cm^{-1} . Measurements of the I^+ signal had a average slope of 2.998 suggesting that those signals were (2+1) REMPI (fig. 3.3), given that no saturation was present. Measurements of CH_3^+ at 17646 cm^{-1} had a average slope of 2.717 which is rounded to 3 and means that those signals were (2+1) REMPI (fig. 3.4). Measurements of CH_3^+ at 17449 cm^{-1} had an average slope of 2.55 but it looks more like a curve than a line which suggests saturation of this signal. This causes a lesser slope so it is rounded to 3 also suggesting those signals were (2+1) REMPI (fig. 3.5).

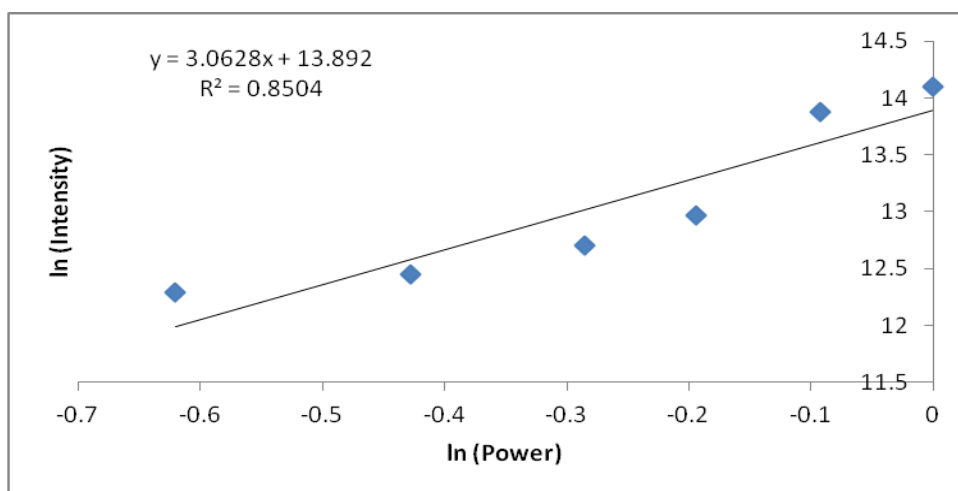


Figure 3.3; A selected power dependence measurement of the I^+ ion signal at 17440 cm^{-1} .

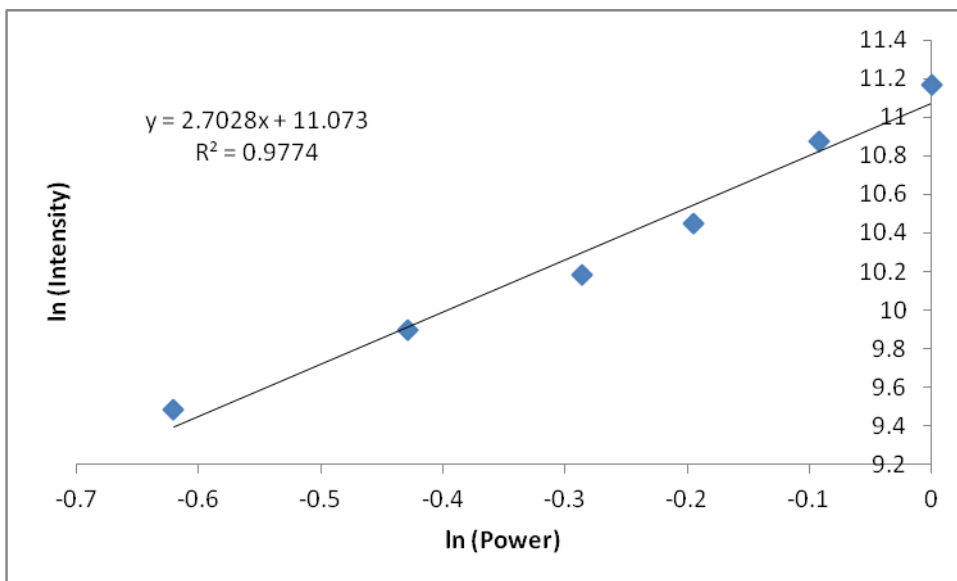


Figure 3.4; A selected power dependence measurement of the CH_3^+ ion signal at 17646 cm^{-1} .

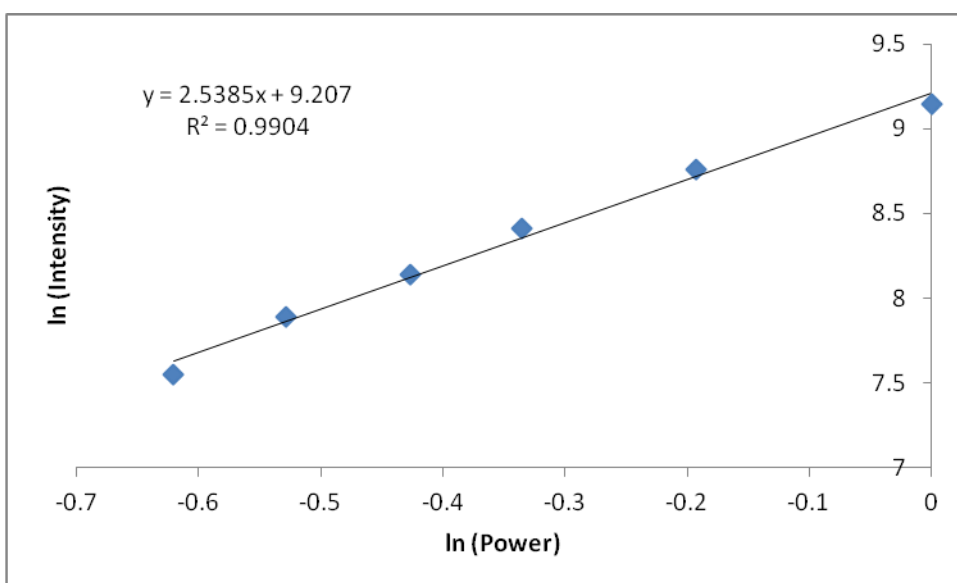


Figure 3.5; A selected power dependence measurement of the CH_3^+ ion signal at 17449 cm^{-1} .

3.3 Ion formation

The neutral fragments in the multiphoton excitation are formed due to excitations of ground state electrons to Rydberg states. After excitation to Rydberg states a curve crossing to repulsive states takes place, followed by dissociation (fig. 3.6). The fragments are then ionized with a unknown number of photons which can be estimated by power dependence measurements.

The most common ions formed are C^+ , CH_3^+ and I^+ . CH^+ and CH_2^+ are also formed but to a lesser extent. This is supported by the 2D-REMPI where the I^+ signal is always present unlike C^+ and CH_3^+ , the other most common ions.

The threshold energy needed to form the different ions has been calculated in table 3.3 using the values from table 3.2 and equation 3.2.

Table 3.2; Bond energies of the single bonds in methyl iodine.^{6,7}

Bond	Energy (cm ⁻¹)
H ₃ C-I	19195.9852
H-H	36450
H-I	24990
C-H	34440

(3.2)

Total energy = (total energy of bonds broken) – (total energy of bonds formed)

⁶ VUV photoionization of (CH₃I)_n (n=1–4) molecules, Jun Chen; Linsen Pei; Jinian Shu; Congxiang Chen; Xingxiao Ma; Liusi Shen; Yunwu Zhang. 2001, Chemical Physics Letters, Vol. 345, P. 57.

⁷ Physical Chemistry – 6th edition, P.W. Atkins. 1998, Oxford University Press, Oxford Melbourne Tokyo.

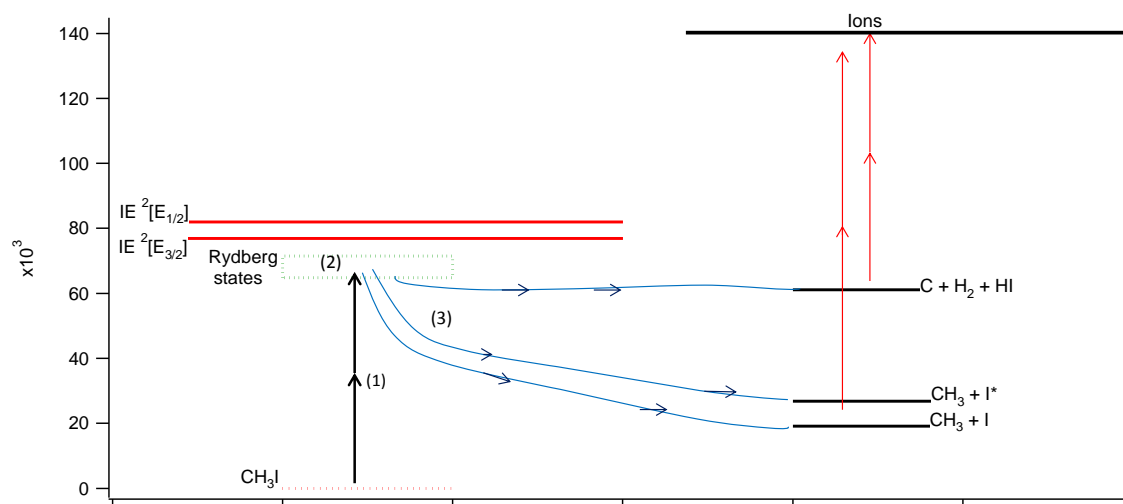


Figure 3.6; Possible dissociation pathways of CH_3I . 1: Excitation to Rydberg states. 2: Curve crossing to repulsive states. 3: Fragmentaion of the CH_3I molecule.

Table 3.3; Ion formation energies calculated using equation 3.2.^{6,7}

Ion	Combination	Energy (cm^{-1})
C^+	$\text{C}+\text{H}+\text{H}+\text{H}+\text{I}$	122516
	$\text{C}+\text{H}+\text{H}+\text{HI}$	97526
	$\text{C}+\text{H}+\text{H}_2+\text{I}$	86066
	$\text{C}+\text{H}_2+\text{HI}$	61076
CH^+	$\text{CH}+\text{H}+\text{H}+\text{I}$	88076
	$\text{CH}+\text{H}_2+\text{I}$	51626
	$\text{CH}+\text{H}+\text{HI}$	63086
CH_2^+	$\text{CH}_2+\text{H}+\text{I}$	53636
	CH_2+HI	28646
CH_3^+	CH_3+I^*	26799
	CH_3+I	19196
I^+	I^*+CH_3	26799
	$\text{I}+\text{CH}_3$	19196

3.4 C⁺ 1D-REMPI

The C⁺ 1D-REMPI spectra show no molecular structure. The C⁺ signal was observed in the 2D-REMPI spectra in the excitation range of 67600 cm⁻¹ – 70200 cm⁻¹ but was recorded for the whole scan region. The C⁺ mass peak was treated with the REMPI integration procedure in IGOR(see page 28). Atomic lines appear in a cluster due to excitation from the 2p orbital to the 3p orbital for three different J's(J=0,1,2). Observed transitions are compared to values (table 3.4) provided by NIST⁸.

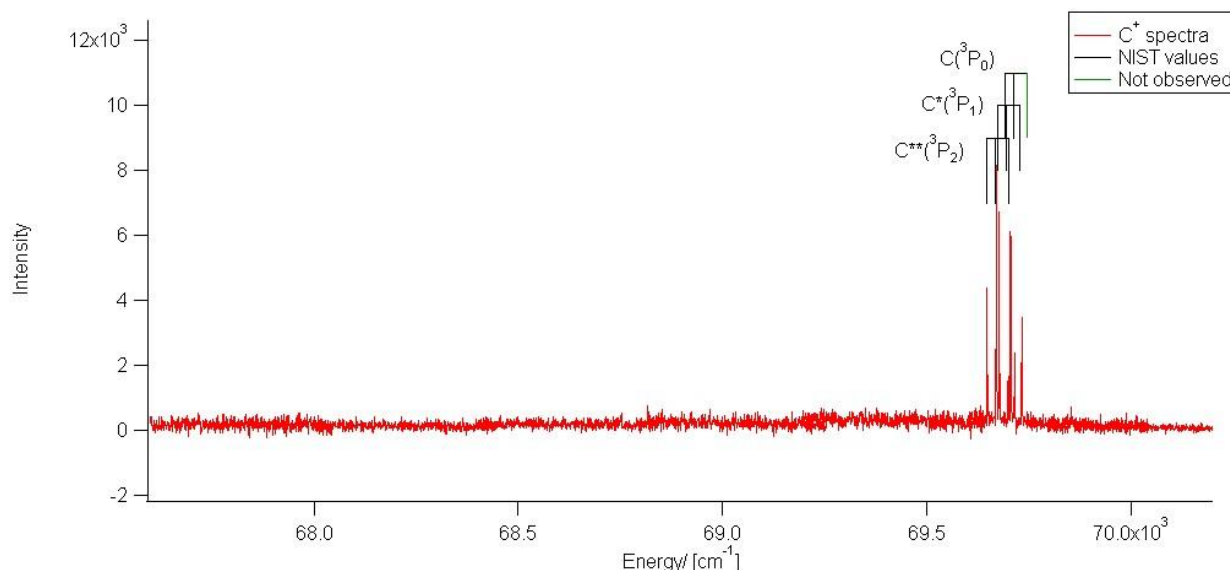


Figure 3.7; 1D-REMPI of C⁺ ion signal in the excitation range where it was present in the 2D-REMPI.

The minimum energy needed for the C atom formation is estimated to be 61405.7 cm⁻¹ (table 3.3). This was calculated using known bond energies of individual bonds that appear in the methyl iodine molecule. Since the lowest calculated energy needed to create a carbon atom is exceeded, carbon atomic lines can be observed as in figure 3.7. Due to the selection rule, allowed transitions are $\Delta l = 0, \pm 2$, where l is the orbital angular momentum. That rule is met as all observed atomic lines are caused by 2p \rightarrow 3p transitions.

Table 3.4; Carbon atomic lines (cm⁻¹) due to (2+n) REMPI of C(2s²2p²; ³P₀), C*(2s²2p²; ³P₁) and C**(2s²2p²; ³P₂)

Configuration	Terms/ 2S'+1X _{J'}	C(2s ² 2p ² ; ³ P ₀)		C*(2s ² 2p ² ; ³ P ₁)		C**(2s ² 2p ² ; ³ P ₂)	
		This work	NIST ⁸	This work	NIST ⁸	This work	NIST ⁸
2s ² 2p3p	³ D ₀	69690.52	69689.48	69673.72	69673.08	69646.01	69646.08
	³ D ₁	69712.95	69710.66	69696.70	69694.26	69667.39	69667.26
	³ D ₂	N/A	69744.03	69731.20	69727.63	69703.04	69700.63

⁸ NIST Atomic Spectra Database (Version 4) [2011, December 9]

As seen in table 3.4, a total of 8 atomic lines were observed and only one allowed atomic line was not observed (fig. 3.8)

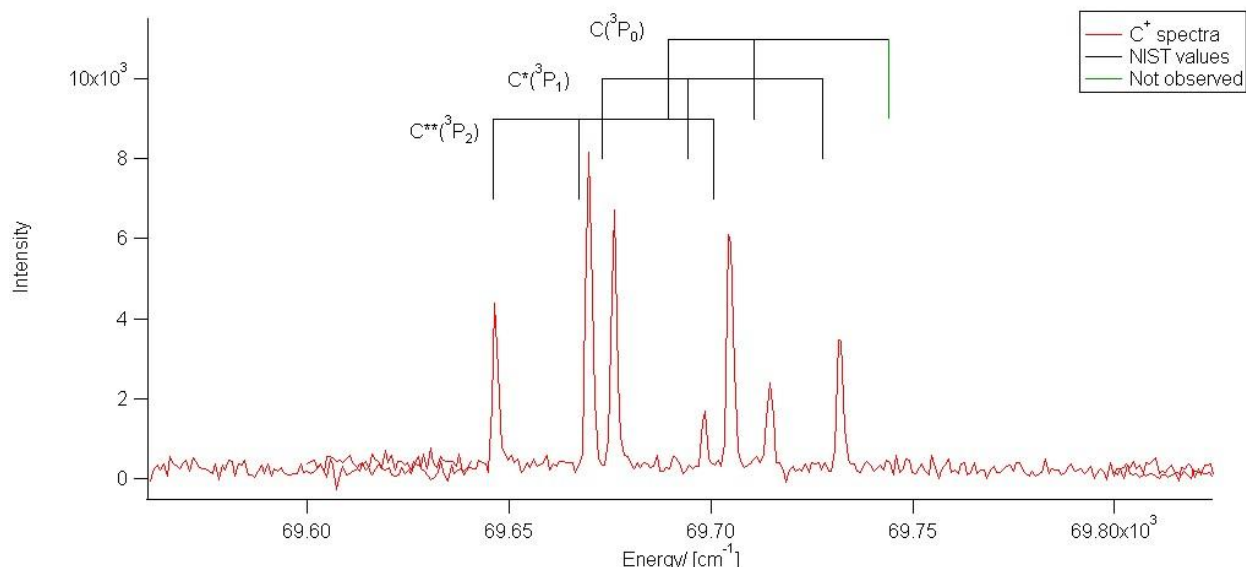


Figure 3.8; Enlarged carbon atomic lines due to (2+n) REMPI of $C(2s^2 2p^2; ^3P_0)$, $C^*(2s^2 2p^2; ^3P_1)$ and $C^{**}(2s^2 2p^2; ^3P_2)$.

There is a small error margin between the measured and previously observed transition energies that can be seen in figure 3.8 where the NIST values are slightly shifted in some cases compared to the measured atomic lines. This error was estimated to be only about 0.005% and is probably due to different experimental designs in recording known transition energies regarding measurement equipments, temperature, pressure and other variables.

The dissociation pathway of CH_3I to form C atoms, hence C^+ ions, is displayed in figure 3.9 where H_2 and HI form as well. Other possibilities are shown but those formations are not thermodynamically possible due to energy requirements. The main conclusion is that the photodissociation of CH_3I form C atoms along with H_2 and HI and are then ionized. Although power dependence measurements were only done for CH_3^+ and I^+ it is assumed that three photons are used to ionize. Further measurements are needed to confirm this.

The relative weakness of the C^+ signals observed is most likely caused by the amount of energy required to create the C fragment compared to the creation of the I and CH_3 fragments.

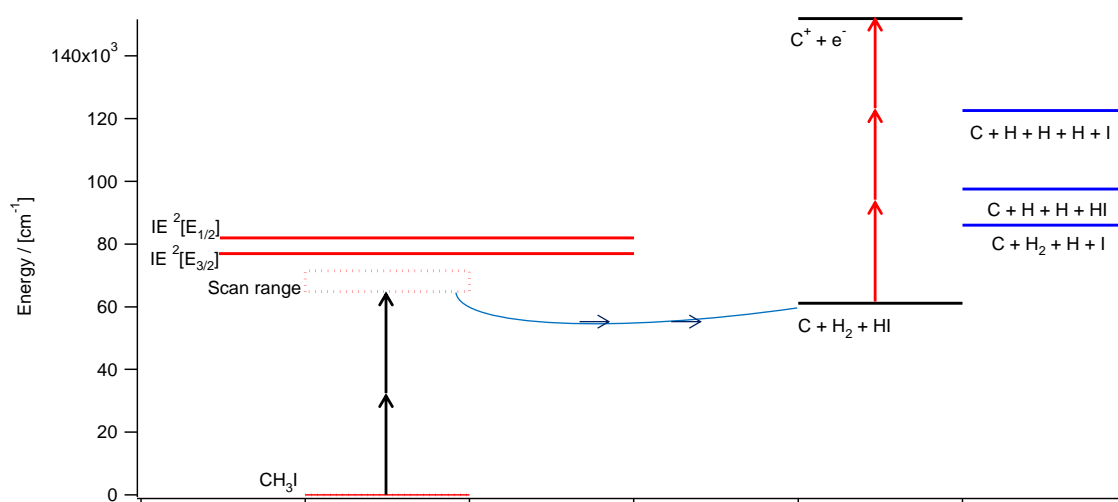


Figure 3.9; A possible dissociation pathway of CH_3I to form C atoms, hence C^+ ions.

3.5 CH₃⁺ 1D-REMPI / Rydberg states

The CH₃⁺ mass peak was present in the 2D-REMPI over the excitation range of 67600 cm⁻¹ to 71480 cm⁻¹. The CH₃⁺ mass peak was treated with the REMPI integration procedure in IGOR(see page 28). The peak could not be observed in the lower energy regions, 64880 cm⁻¹ – 67600 cm⁻¹. This is most likely due to diminished laser power. The CH₃⁺ 1D-REMPI displayed continuous molecular structure (fig. 3.12b). Allowed transitions in the two-photon excitation are $\Delta l = 0, \pm 2$, however, in the molecular absorption of methyl iodine, the non-bonding 5p π electron is first believed to be excited probably to an antibonding σ^* orbital in the C-I bond. This results in transitions to ns Rydberg states in methyl iodine in two-photon excitation.⁹

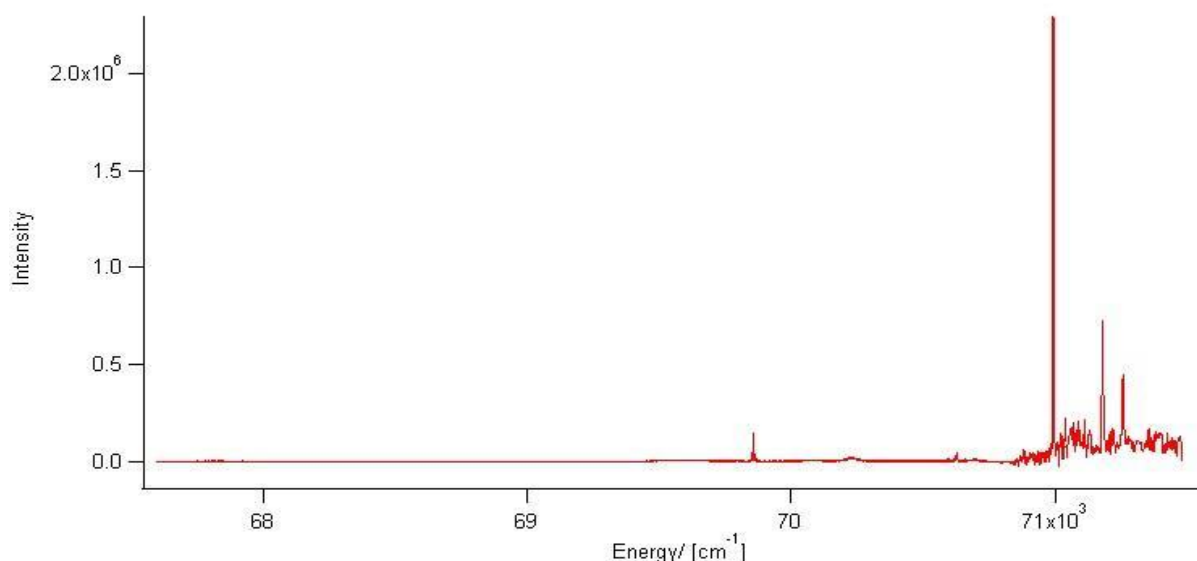


Figure 3.10; Total CH₃⁺ 1D-REMPI spectra, see also figs. 3.12 and 3.13.

The CH₃⁺ 1D-REMPI spectrum (fig. 3.11) in the scan range of 70840 cm⁻¹ – 71480 cm⁻¹ displayed large sharp lines and was more noisy than other regions. This is because of saturation of the iodine signal in this region. These lines are iodine atomic lines. Comparison between the 1D-REMPI spectra of I⁺ and CH₃⁺ is shown in figure 3.11. It can be seen that although not all the atomic lines are observed in both spectra, the strongest lines are. The lowest energy peak is due to the I*(5s²5p⁵; ²P_{1/2}) → 5s²5p⁴(¹D₂)6p transition and the other peaks are due to I*(5s²5p⁵; ²P_{1/2}) → 5s²5p⁴(³P₂)8p transitions (see table 3.8).

⁹ Resonance enhanced multiphoton ionization photoelectron spectroscopy on nanosecond and picosecond time scales of Rydberg states of methyl iodide. M. R. Dobber; W. J. Buma; and C. A. de Lange. 1993 Journal of Chemical Physics, Vol. 99, No. 2, P. 836.

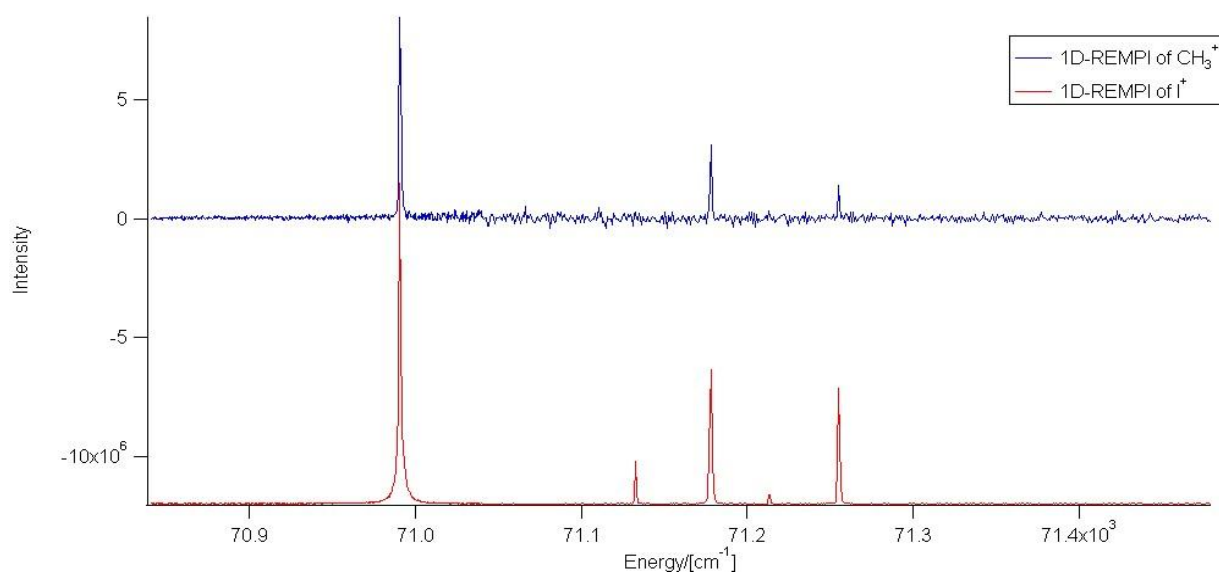


Figure 3.11; Comparison of the 1D-REMPI of I^+ and CH_3^+ .

The broad continuous peaks of the 1D-REMPI of CH_3^+ were assigned to Rydberg state transitions using previous assignments for comparison. This was done by calculating quantum defects of each state in previous measurements using equation 1.1. Calculations were also done by using iodine excitation energies provided by NIST⁸ assuming the iodine atom to be dominating in the defects of the molecule.

In equation 1.1 E is the transition energy, IE is the ionization energy, R_H is the Rydberg constant, n is the principal quantum number and δ is the quantum defect. Assignment of each peak was done by calculating its quantum defect at different principal quantum numbers and then compared with quantum defects at each Rydberg state in previous measurements.^{9,10,11} This was not accurate for all peaks but was good enough to assign each peak. The calculated quantum defect range can be seen in table 3.5.

Table 3.5; Calculated quantum defects using previous measurements of methyl iodine and iodine transitions along with assumed defects using individual measurements of previous measurements.^{9,10,11}

	Calculated Quantum defect [δ]		Assumed Quantum defect [δ]	
	Maximum	Minimum	Maximum	Minimum
s	4.06	3.98	4.07	3.95
p	3.62	3.45	3.62	3.45
d	2.55	1.9	2.24	2.08

The calculated quantum defect for the d-orbital transitions in table 3.5 has a very wide range and the largest numbers all came from iodine transitions. Therefore those

¹⁰ Medium and high resolution vacuum UV photoabsorption spectroscopy of methyl iodide (CH_3I) and its deuterated isotopomers CD_3I and CH_2DI , 2009

¹¹ VUV spectroscopy of CH_3Cl and CH_3I , 2007.

values were disregarded. In the assignments the largest values for the d-orbital were overlooked and it was estimated to be between about 2.2 and 2.08. A similar approach was used in assigning the s-orbital transitions but in reverse to widen the range. That was done because individual defects from previous measurements^{9,10,11} were often well outside the s-orbital defect range. The actual range used for the s-orbital transitions was 4.07 to 3.95. The p-orbital transition defects were left unchanged since they did all fit within the individual defect range. Figures 3.12 a and b show the possible range of each Rydberg state in the 1D-REMPI of CH_3^+ .

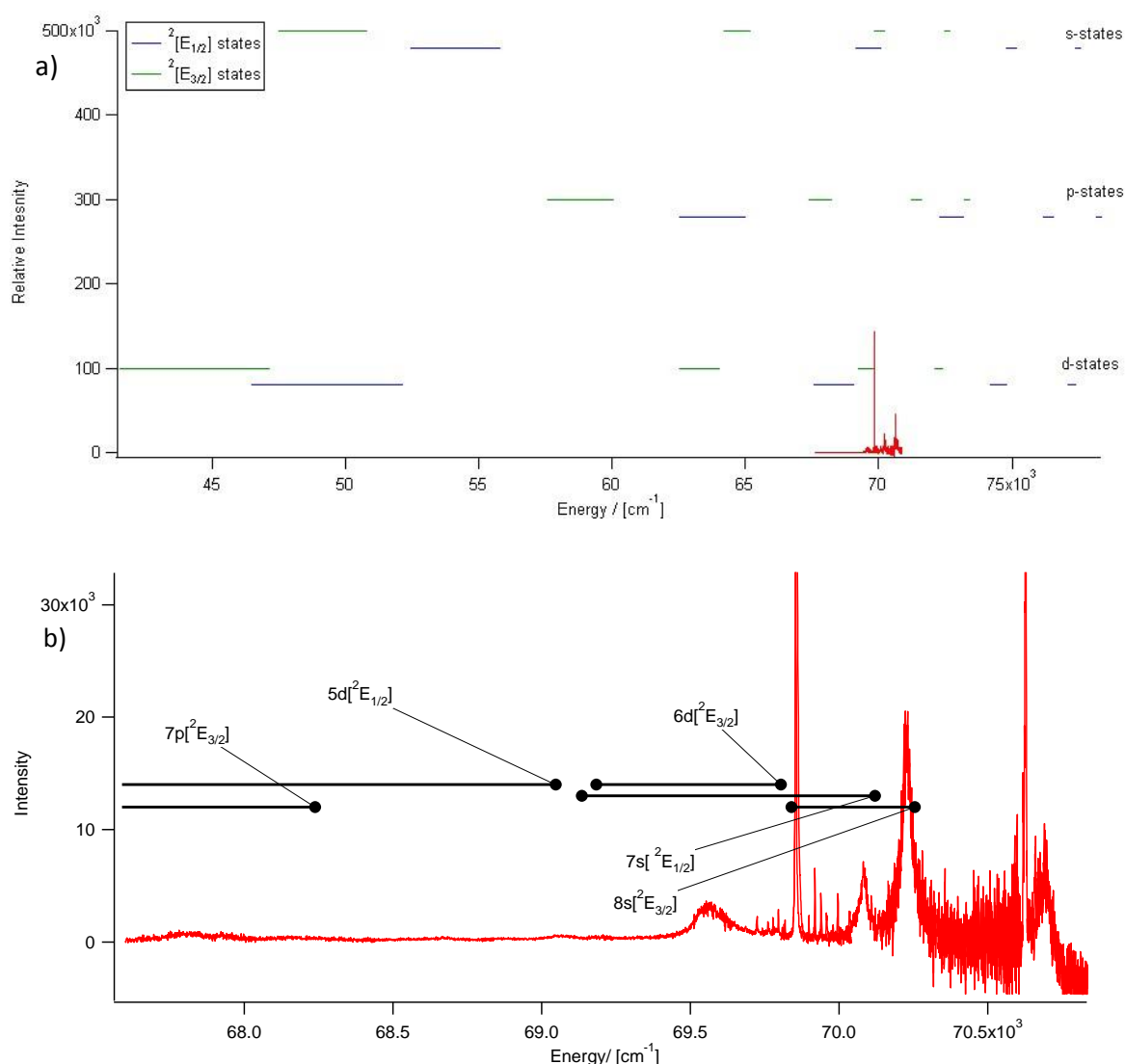


Figure 3.12; a) Overall view of possible ranges for Rydberg state transitions. b) Possible ranges of Rydberg state transitions in the scan range of the 1D-REMPI for CH_3^+ .

Although ns, np and nd Rydberg state transitions all can be in the excited region, most of the peaks have been previously assigned as ns Rydberg states. This is due to the previously discussed excitation of a non-bonding $5p\pi$ electron transition via the anti-bonding σ^* orbital in the C-I bond. The final excitation involves from σ^* to ns transitions.

The np Rydberg state transitions have been previously observed as weaker peaks⁹ and fit to the observed 1D-REMPI and the Rydberg state ranges in figure 3.12. Along with the Rydberg state transitions observed there are two suspected vibrational bands.

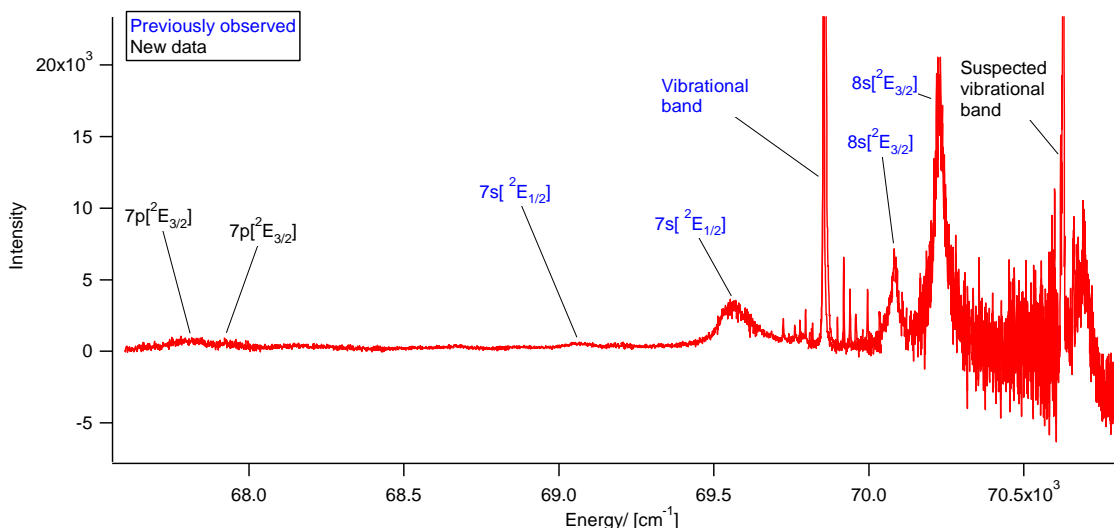


Figure 3.13; Assigned Rydberg state transition peaks in the 1D-REMPI of CH_3^+ .

Five of the eight peaks observed, and counting the vibrational band as single peaks marked in figure 3.13, have been previously observed and assigned. Summary of the observed peaks is shown in table 3.6 and comparison with the previously observed peak positions.

Table 3.6; Experimental CH_3^+ peak positions compared with previously observed peaks.

Experimental position/[cm ⁻¹]	Previously observed position/[cm ⁻¹] ^{9,10,12}	Excitation	Rydberg state
70624.06	-	Vibrational	-
70217.65	70219	Rydberg	8s ² E _{3/2}
70077.02	70074	Rydberg	8s ² E _{3/2}
69848.97	69853.44	Vibrational	-
69560.26	69548	Rydberg	7s ² E _{1/2}
69097.43	69125	Rydberg	7s ² E _{1/2}
67940.1	-	Rydberg	7p ² E _{3/2}
67803.81	-	Rydberg	7p ² E _{3/2}

The suggested dissociation pathway of CH_3I to form CH_3 , hence the CH_3^+ ion is shown in figure 3.14. Two photons excite electrons to Rydberg states. Curve crossing followed by a repulsive state leads to dissociation. Then CH_3 fragment is ionized with three photons, as the power dependance measurements suggest. The vibrational states $K=0$

and $K=1$ in figure 3.14 are assumed to be excitations of the methyl radical rather than the CH_3^+ ion¹² and are discussed in more detail in chapter 3.8.

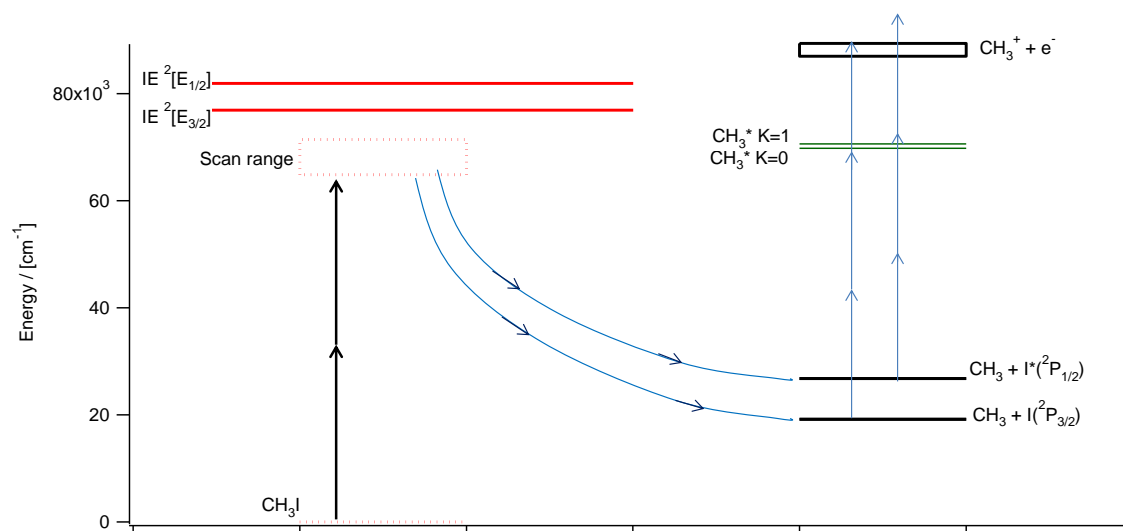


Figure 3.14; Suggested pathway of the dissociation of CH_3I to form the CH_3^+ ion.

¹² Rotational structure and predissociation dynamics of the methyl $4p_z$ ($v=0$) Rydberg state investigated by resonance enhanced multiphoton ionization spectroscopy, 1988

3.6 CH₃* Vibrational bands

Two similar spectra were observed at 69848.97 cm⁻¹ and 70626.462 cm⁻¹ (fig. 3.15). Both show strong main peaks with weak peaks on both sides. The higher energy spectrum shows smaller spacing between peaks. The spectrum observed at a lower energy has been previously observed and found to be a vibrational band from the umbrella movement of the flat CH₃* radical.¹²

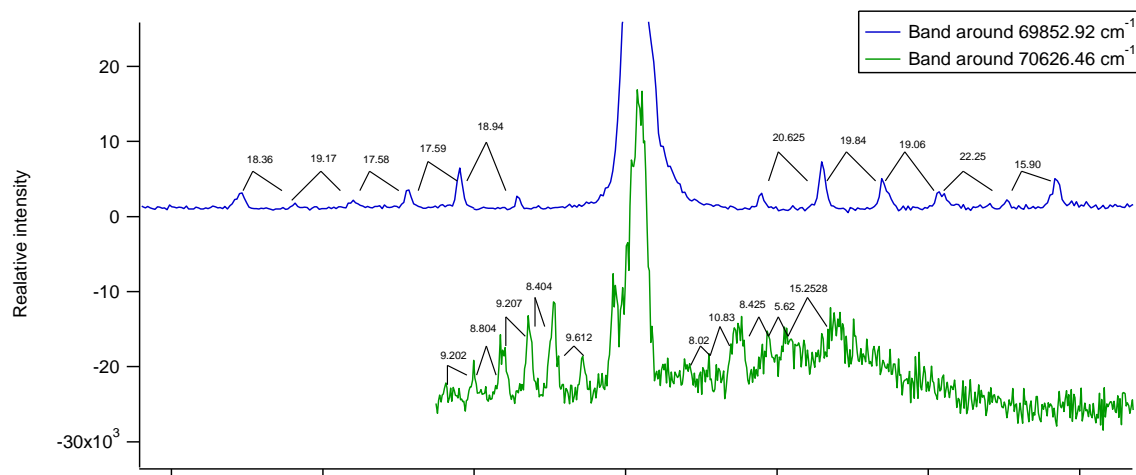


Figure 3.15; Comparison of the suspected vibrational peaks at 69848.97 cm⁻¹ and 70626.46 cm⁻¹.

No previous observation of the spectrum at 70626.462 cm⁻¹ has been reported but the spacing in energy between the two spectra, 777.49, suggests that this is due to an out-of-plane-large-amplitude (OPLA) 4p²a₂ v₂ excited vibrational transition.⁸ Using equation 3.3, which is the same equation derived from the least squares analysis of the lower energy spectrum¹², parameters for the higher energy spectrum could be roughly estimated. This was done in IGOR using a procedure found in the appendix (page 33). Using a simple trial and error to be a reasonable match of calculated and measured peaks was found (fig. 3.16).

(3.3)

$$v = v_0 + \Delta CK^2 - \Delta D_K K^4 + \left[B'N'(N'+1) - B'K^2 - D'_N N'^2(N'+1)^2 \right] - B''N''(N''+1) - B''K^2 - D''_K N''^2(N''+1)^2 - D''_{NK} N''(N''+1)K^2]$$

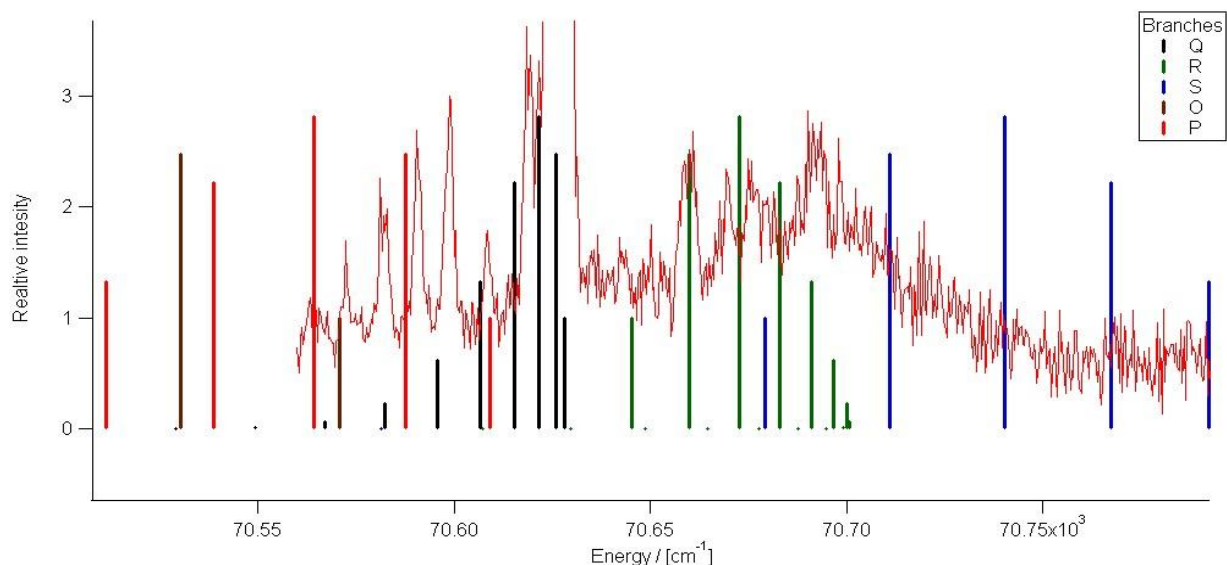


Figure 3.16; A sample of the trial and error fitting in estimating rotational constants.

As seen in figure 3.16 the calculated peaks do not match the intensity of the measured peaks but these intensities are not accurate in any way, therefore only the peaks positions should be considered. Parameters used in the fit procedure were the rotational constants, B' and D' , and the quantum number, K . Results are shown in table 3.7.

Table 3.7; Fit parameters for vibrational bands at 69848.97 cm^{-1} and $70626.462 \text{ cm}^{-1}$.

Ground state	Parameter values/[cm^{-1}]	Excited state $K=0$	Parameter values/[cm^{-1}]	Excited state $K=1$	Parameter values/[cm^{-1}]
B''	9.57789	B'	9.90 ± 0.01	B'	8.5
$D''_N * 10^4$	7.699	$D'_N * 10^4$	10.7 ± 1.2	$D'_N * 10^4$	10.7 ± 1.2
$D''_{NK} * 10^4$	-1.358	$D'_{NK} * 10^4$	-21.2 ± 1.8	$D'_{NK} * 10^4$	-21.2 ± 1.8
		ν_0	69853.44 ± 0.13	ν_0	70627.2

The band needs further investigation for a more precise analysis. The peaks significance was not realized until after measurements were finished and no proof of its reproducibility is available.

3.7 I⁺ 1D-REMPI

The iodine mass signal was observed in all the recorded spectra range and was treated with the REMPI integration procedure in IGOR(see page 28). No molecular structure was observed in the 1D-REMPI spectra, only atomic lines. A total of 19 atomic lines were observed in the scan range(table 3.8).

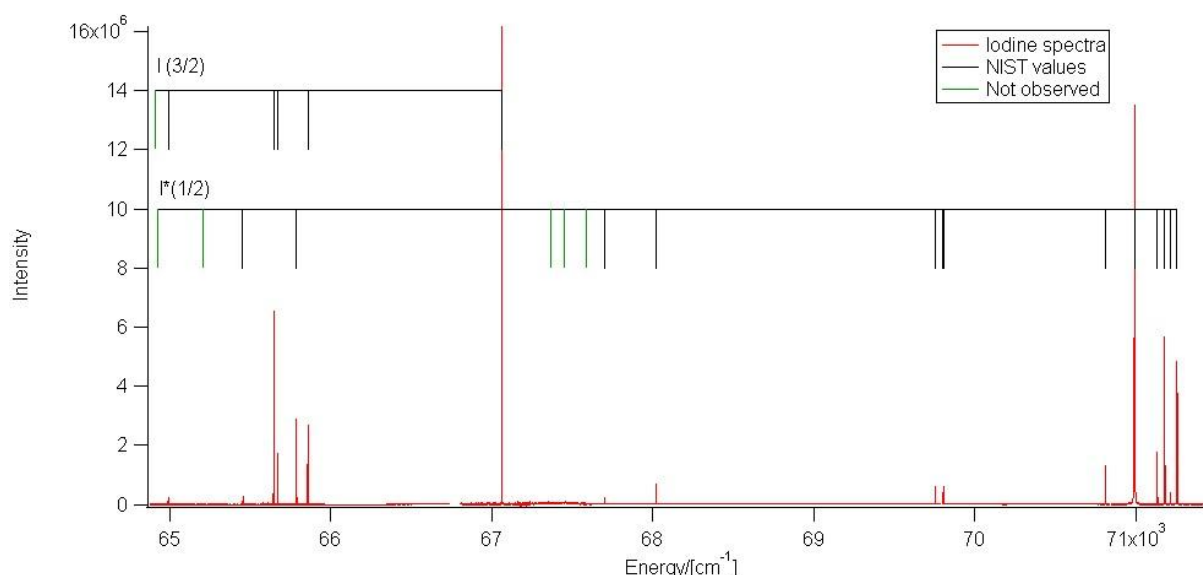


Figure 3.17; Iodine atomic lines (cm^{-1}) due to $(2+n)$ REMPI of $\text{I}(5s^25p^5;^2P_{3/2})$ and $\text{I}^*(5s^25p^5;^2P_{1/2})$ along with previously observed transitions.

A total of 6 allowed transitions were not observed in the scans as can be seen in figure 3.17 and table 3.8. Due to the selection rule, $\Delta J = 0, \pm 1, \pm 2$, there were 5 nonallowed transitions in the scan range that were not observed. The two photon excitation makes only $np \rightarrow n'p$ and $np \rightarrow n'f$ transitions possible due to the selection rule $\Delta l = 0, +2$, where l is the orbital angular momentum.

As previously discussed, in the high energy scans ($70840\text{cm}^{-1} - 71480\text{cm}^{-1}$) a saturation effect due to many strong iodine atomic lines appearing over a short range affected other 2D-REMPI peaks. This caused the other 1D-REMPI spectra to display iodine atomic lines (fig. 3.11).

The fact that no observable molecular structure was present in the iodine spectra suggests that methyl iodine readily dissociates to a methyl radical and a iodine atom. Dissociation pathways previously reported⁹ discuss the excitation of a non-bond electron to an anti-bonding orbital in the carbon-iodine bond being the first excitation, this causes the molecule to enter a repulsive state where its dissociation is very fast and happens almost instantly and forms CH_3 and I , similar to a CH_3Br research¹³ which follows the CH_3X dissociation ($\text{X}=\text{halogen}$). This is supported in these measurement by the fact that the iodine signal is detected in every scan since iodine ionizes at a lower energy than CH_3 .

¹³ Two-Dimensional $(2+n)$ REMPI of CH_3Br : Photodissociation Channels via Rydberg States, 2010.

The suggested dissociation pathway of CH_3I to form a I^+ is shown in figure 3.18 where the first excitation causes the formation of CH_3 , I and I^* . I^* is spin orbit excited $\text{I}(^2\text{P}_{1/2})$. I and I^* are then ionized with three photons as the power dependence measurements suggest. The formation of I^{**} , a Rydberg excited I atom, is dismissed by its energy requirement that is higher than the scan range. Since Rydberg state transitions are observed in the CH_3^+ 1D-REMPI the I^+ 1D-REMPI should also have Rydberg state transitions from the same dissociations but it is dominated by large atomic lines. This can be explained by forming I^+ in two different pathways. The first pathway is the formation of a $\text{CH}_3^+ \text{I}^-$ ion pair that enters a repulsive state and the I fragment from that pair is then ionized. The second pathway is the same as for CH_3^+ , where CH_3I is excited to a Rydberg state and from there it enters a repulsive state. The I fragment is then ionized.

The relative size of the I^+ signal in the 2D-REMPI spectra suggests that the ion pair pathway may be the dominant dissociation path but more research is needed to confirm this conclusion. The reason for the molecular structure not being observed in the 1D-REMPI of I^+ could be caused by long tails from the atomic lines masking the smaller peaks.

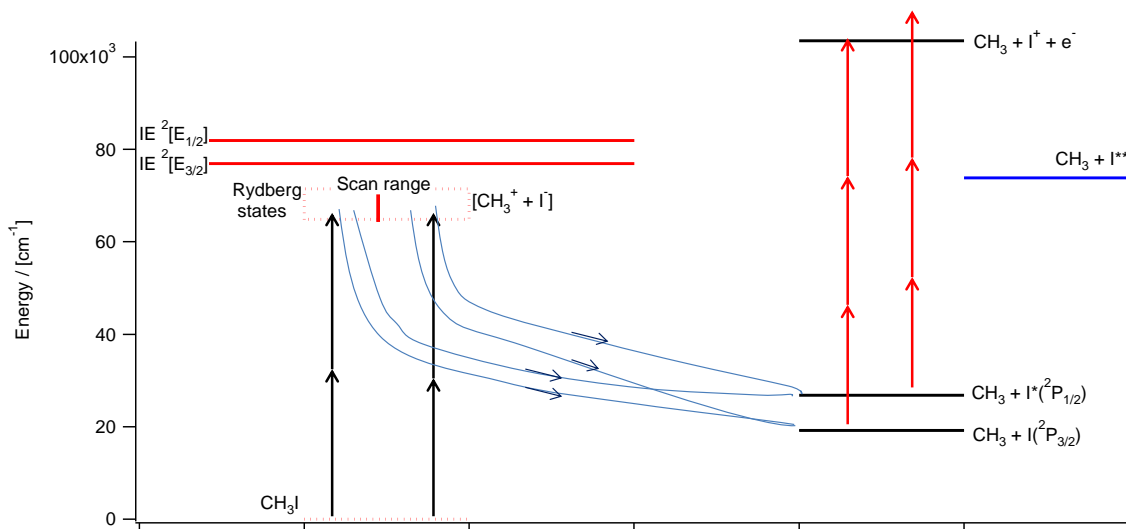


Figure 3.18; Suggested dissociation pathways of CH_3I to form I^+ ions. Two possible pathways are shown: The dissociation from Rydberg state transitions and the dissociation from ion pair formations.

Table 3.8; Iodine atomic lines (cm^{-1}) due to (2+n) REMPI of $I(5s^25p^5;^2P_{3/2})$ and $I^*(5s^25p^5;^2P_{1/2})$.

Confiuration	terms/ $2S'+1X_J'$	$I(5s^25p^5;^2P_{3/2})$		$I^*(5s^25p^5;^2P_{1/2})$	
		This work	NIST ⁸	This work	NIST ⁸
$5s^25p^4(^3P_2)6p$	$^2[2]_{5/2}$	N/A	64906.29		
	$^2[2]_{3/2}$	64990.05	64989.994		
	$^2[3]_{5/2}$	65644.718	65644.476		
	$^2[3]_{7/2}$	65670.083	65669.988		
	$^2[1]_{1/2}$	65856.962	65856.960		
	$^2[2]_{3/2}$	67061.600	67062.130		
$5s^25p^4(^3P_1)6p$	$^2[2]_{5/2}$			N/A	64926.21
	$^2[2]_{3/2}$			N/A	65204.19
	$^2[1]_{3/2}$			65453.774	65451.63
	$^2[1]_{1/2}$			65786.858	65784.21
$5s^25p^4(^3P_2)7p$	$^2[2]_{5/2}$			N/A	67362.67
	$^2[2]_{3/2}$			N/A	67446.54
	$^2[3]_{5/2}$			N/A	67588.37
	$^2[3]_{7/2}$			Nonallowed	
	$^2[1]_{1/2}$			67703.36	67700.1
	$^2[1]_{3/2}$			68021.61	68018.46
$5s^25p^4(^3P_2)4f$	$^2[2]_{3/2}$			69756.6	69753.67
	$^2[2]_{5/2}$			69759.38	69756.62
	$^2[5]_{11/2}$			Nonallowed	
	$^2[5]_{9/2}$			Nonallowed	
	$^2[1]_{1/2}$			69801.49	69801.39
	$^2[1]_{3/2}$			69803.87	69803.81
$5s^25p^4(^1D_2)6p$	$^2[1]_{3/2}$			70812.499	70812.28
				70812.902	70812.28
				70813.707	70812.28
	$^2[3]_{5/2}$			70990.719	70989.6
	$^2[3]_{7/2}$			Nonallowed	
$5s^25p^4(^3P_2)8p$	$^2[2]_{5/2}$			71132.920	71129.26
	$^2[1]_{5/2}$			71177.87	71177.14
	$^2[1]_{3/2}$			71213.22	71212.47
	$^2[3]_{7/2}$			Nonallowed	
	$^2[3]_{5/2}$			71255.85	71251.78

4 Conclusions

CH₃I was analyzed by the (2+n) REMPI-TOF technique over the excitation region 64880 cm⁻¹ to 71480 cm⁻¹. The main ion peaks observed were due to C⁺, I⁺ and CH₃⁺ and they were further analyzed to yield 1D-REMPI spectra. The ion peaks of CH⁺ and CH₂⁺ were also observed over a narrow range, but those were considered to be incomplete and were not analyzed further.

The C⁺ signal displayed eight atomic lines that were compared with known values.⁸ No continuous signal was observed which could be assigned to the CH₃I molecular absorption. The signal was relatively weak, and was not observed in the lower energy regions. C⁺ ion signals are believed to be due to the dissociation of CH₃I to C, H₂ and HI since other fragment formation is considered to be thermodynamically impossible from calculations of bond energies.

The CH₃⁺ 1D-REMPI spectra display broad molecular absorption bands. Both Rydberg excitations and suspected CH₃* vibrational transitions were observed. The Rydberg state spectra do not follow the selection rule regarding two-photon excitation which is believed to be because of the excitation path of CH₃I, which occurs from the non-bonding p-orbital via anti-bonding orbital in the carbon-iodine bond followed by an excitation orbital to a ns-orbital.⁹ Weaker peaks due to np Rydberg states were also observed but their relative weakness suggests that the corresponding transitions are less likely.

One of two vibrational bands observed in the CH₃⁺ 1D-REMPI was assigned based on a earlier experiment.¹² The other band has not been observed before and needs to be further investigated to assure its assignment.

The I⁺ signal displayed only strong, sharp atomic lines. These lines were compared to known values.⁸ No broad molecular peaks were observed. Since Rydberg state transitions are observed in the CH₃⁺ 1D-REMPI they are also present in the I⁺ 1D-REMPI but are masked by the larger atomic lines and their tails. This suggests that the dissociation of CH₃I to form I atoms, hence I⁺ ions, has two pathways. The first pathway is the excitation of CH₃I to Rydberg states. Curve crossing followed by a repulsive state then leads to the dissociation of CH₃I to CH₃ and a I atom which is then ionized. The second pathway, believed to be dominant, is the formation of a CH₃⁺ I ion pair which enters a repulsive state and the I fragment is then ionized.

References

- (1) *Environmental Chemistry – 4th edition*. **Baird, C.; Cann, N. 2008.** 2008, W. H. Freeman and Company.
- (2) *California under fire for approving controversial pesticide*. **Rebecca Trager 2011.** 2011 Royal Society of Chemistry.
- (3) *Multiphoton Spectroscopy, Applications*. **Michael NR Ashfold, Colin M Western 1999.** 1999 Elsevier Ltd., Vol. 2, P. 1424.
- (4) *Photofragmentations, State Interactions and Energetics of Rydberg and Ion-pair states: Two Dimensional Resonance Enhanced Multiphoton Ionization of HBr via singlet-, triplet-, $\Omega = 0$ and 2 states*. **Jingming Long, Helgi Rafn Hróðmarsson, Huasheng Wang, Ágúst Kvaran 2012.**
- (5) *Effect of Dimers on the Temperature-Dependent Absorption Cross Section of Methyl Iodide*. **Gabriela C. G. Waschewsky, Robert Horansky, and Veronica Vaida 1996.** 1996, Journal of Physical Chemistry, Vol. 100, No. 28, P. 11559.
- (6) *VUV photoionization of $(CH_3I)_n$ ($n=1-4$) molecules*. **Jun Chen; Linsen Pei; Jinian Shu; Congxiang Chen; Xingxiao Ma; Liusi Shen; Yunwu Zhang 2001.** 2001, Chemical Physics Letters, Vol. 345, P. 57.
- (7) *Physical Chemistry – 6th edition*. **P.W. Atkins 1998.** 1998, Oxford University Press, Oxford Melbourne Tokyo.
- (8) *NIST Atomic Spectra Database (Version 4) [2011, December 9]*, [Online]. Available: <http://www.nist.gov/pml/data/asd.cfm>. National Institute of Standards and Technology, Gaithersburg, MD.
- (9) *Resonance enhanced multiphoton ionization photoelectron spectroscopy on nanosecond and picosecond time scales of Rydberg states of methyl iodide*. **M. R. Dobber; W. J. Buma; and C. A. de Lange 1993.** 1993 Journal of Chemical Physics, Vol. 99, No. 2, P. 836.
- (10) *Medium and high resolution vacuum UV photoabsorption spectroscopy of methyl iodide (CH_3I) and its deuterated isotopomers CD_3I and CH_2DI . A Rydberg series analysis*. **R. Loch, B. Leyh, H.W. Jochims, H. Baumgärtel 2009.** 2009, Chemical Physics, Vol. 365, P. 109.
- (11) *VUV spectroscopy of CH_3Cl and CH_3I* . **S. Eden, P. Limao-Vieir, S.V. Hoffmann, N.J. Mason 2006.** 2007 Chemical Physics, Vol. 331, P. 232.
- (12) *Rotational structure and predissociation dynamics of the methyl $4p_z$ ($v=0$) Rydberg state investigated by resonance enhanced multiphoton ionization spectroscopy*. **John F. Black, Ivan Powis 1988.** 1988 Journal of Chemical Physics, Vol. 89, P. 3986.

(13) *Two-Dimensional (2+n) REMPI of CH₃Br: Photodissociation Channels via Rydberg States.* **Kvaran, Á; Wang, H.; Matthíasson, K. 2010.** 2010, Journal of Physical Chemistry, Vol. 114, No. 37, P. 9991.

Appendix

Igor codes

Mass axis calibration

```
#pragma rtGlobals=1          // Use modern global access method.
macro Use_cursor()
showinfo
variable tureorfalse
tureorfalse=exists("massreference")
if (tureorfalse==1)
killwaves massreference
killwaves masspoint
make/n=0 massreference
make/n=0 masspoint
else
make/n=0 massreference
make/n=0 masspoint
endif
endmacro
function getwavenum(wavenam)    //this function is used to find the number of wave
string wavenam
variable/G wavenum
sscanf wavenam,"wave%f", wavenum
end
macro Add_reference(mass)
variable mass
prompt mass,"Please input its mass:"
variable x1
x1=hcsr(A)
insertpoints 0,1,massreference
insertpoints 0,1,masspoint
massreference[0]=mass
masspoint[0]=x1
endmacro
macro Produce_massaxis( ) //delete masspoints prompt
variable masspoints
//prompt masspoints,"Please input the number of mass spectra points"
string wavenamfromcsr=csrwave(A)
masspoints=umpnts($wavenamfromcsr)
variable tureorfalse
tureorfalse=exists("constants")
if (tureorfalse==1)
killwaves constants
make/d/n=2 constants={0,0}
else
make/d/n=2 constants={0,0}
endif
funcfit /h="00" massfit constants masspoint /x=massreference /d
display masspoint vs massreference
modifygraph mode(masspoint)=3, rgb=(0,0,0)
appendtograph fit_masspoint
tureorfalse=exists("massaxis")
```

```

if (tureorfalse==1)
else
make/n=(masspoints) massaxis
endif
massaxis=((x-constants[1])/constants[0])^2
variable i=0
if(constants[1]>0)
do
massaxis[i]=-massaxis[i]
i+=1
while(i<constants[1])
endif
doalert 0, "Ok! You get a mass axis. Its name is 'massaxis' ! Now you can change x with new axis
:)"
killwaves constants
killwaves W_sigma
endmacro
function massfit(constants, m):FitFunc
wave constants
variable m
return constants[0]*m^0.5+constants[1]
end

```

REMPI Intergration

```

#pragma rtGlobals=1          // Use modern global access method.
menu "Macros"
"REMPI_Integrate"
end
macro REMPI_Integrate(wavestart,waveend,finallyname)
string wavestart
Prompt wavestart, "Beginning Wavename:", popup, WaveList(";",",","")
string waveend
Prompt waveend, "Ending Wavename:", popup, WaveList(";",",","")
string finallyname
Prompt finallyname, "Wavename:"
variable startpoint
variable endpoint
variable/G wavenum          //getthe number in input wavename and global
string wavenameconstant    //set "wave" as a string constant
wavenameconstant="wave"
variable startwave
variable endwave
variable wavedeta
variable eachwaveintegrate
string wavenam
variable x1
variable x2
variable detax
x1=pcsr(A)
x2=pcsr(B)
if (x1<x2)
startpoint=x1
endpoint=x2
else

```



```

startpoint=x2
endpoint=x1
endif
detax=endpoint-startpoint
getwavenum(wavestart)      //use "getwavenum" function to get the number
startwave=wavenum
getwavenum(waveend)
endwave=wavenum
wavedeta=endwave-startwave+1 //obatin the delta between start wave and end wave
make/O/N=(wavedeta) $finallyname //make a new wave, and name as user defined
variable i
i=0
variable yaveragevalue
do
wavenam=wavenameconstant+num2str(i+startwave)
if (mean($wavenam,startpoint-2,startpoint+2)<mean($wavenam,endpoint-2,endpoint+2))
yaveragevalue=mean($wavenam,startpoint-2,startpoint+2)
else
yaveragevalue=mean($wavenam,endpoint-2,endpoint+2)
endif
$finallyname[i]=area($wavenam,startpoint,endpoint)-detax*yaveragevalue
i+=1
while(i<wavedeta)
print " O k ! You get the wave name is: "+finallyname
display $finallyname

```

Energy Calibration

```

#pragma rtGlobals=1          // Use modern global access method.
#pragma rtGlobals=1          // Use modern global access method.
menu "Macros"
submenu "ECalibration"
  "ECalibration"           //To calibrate the spectrum according to power changing during one
  scanning.
  "CancelECali"           //To cancel the last Ecalibration.
  "ChangeScale"           //Using one standard power to unify all spectra, eg. power and photons.
end
submenu "Calibrate"
  "Calibrate"             //To connect the ending of the spectrum to the beginning of next spectrum
  for two different scannings.
  "Back"                  //To cancel the last calibration.
end
end
//you need to use "A cursor" to get the wave name which you want to calibrate!!
macro ECalibration(power_start, power_end,nn)
Variable power_start
Prompt power_start, "Power in the beginning : "
Variable power_end
Prompt power_end, "Power in the end : "
variable nn
prompt nn, "Number of photons : "
string wavey
string wavex
wavey=CsrWave(A)
wavex=CsrXWave(A)

```

```

variable lengthofwave
lengthofwave=numpts($wavex)
variable kslope
variable valueb
kslope=(power_end-power_start)/($wavex[lengthofwave]-$wavex[0])
valueb=power_start-kslope*$wavex[0]
make/O/N=(lengthofwave) powerline
powerline=valueb+kslope*$wavex
powerline=(1/(powerline^nn))*(power_start^nn)
$wavey=$wavey*powerline
print "-----"
print "Power at start :",power_start,"mW"
print "Power at end :",power_end,"mW"
print "Numbers of photons:", nn
print "Calibrated wave name is :", wavey
print "-----"
end
macro CancelECali()
doalert 1,"Are you sure you cancel last calibration?"
if (V_flag==1)
string wavey
wavey=CsrWave(A)
$wavey=$wavey/powerline
killwaves powerline
print "You cancel the last energy calibration"
endif
end
macro ChangeScale(power0)
variable power0
string wavechange
variable apositionvalue
variable bpositionvalue
apositionvalue=vcsr(A) //you need to use "A cursor" to get the wave name and
determinate Ie value!!
bpositionvalue=vcsr(B) // and use cursor B to determinate the value of Io.
wavechange=CsrWave(A)
// $wavechange=bpositionvalue-apositionvalue+$wavechange
//print "B:", apositionvalue,"A:", bpositionvalue
//print "Calibrated wave name is :", wavechange
//print wavechange,"+=", apositionvalue,"-", bpositionvalue,""
// $wavechange=$wavechange*(bpositionvalue/apositionvalue)
//print "B:", apositionvalue,"A:", bpositionvalue
$wavechange=((9/power0)^2)*$wavechange // Here you can set the value of the
standard power and the number of photons.
//print "Calibrated wave name is :", wavechange
//print wavechange,"*=", bpositionvalue,"/", apositionvalue
print wavechange, "*(9/", power0, ")^2"
end
macro Calibrate()
string wavechange
string wavechangex
variable Io
variable Ie
Ie=vcsr(A)
Io=vcsr(B)

```

```

wavechange=CsrWave(A)
wavechangex=CsrXWave(A)
variable lengthofwave
lengthofwave=numpts($wavechangex)
make/O/N=(lengthofwave) backupwave
backupwave=$wavechange
variable aa
variable bb
variable nn
variable cc
nn=2 //set the number of photons
cc=($wavechangex[0])^nn
aa=((Ie/Io-1)/(abs((hcsr(A))^nn-cc)))
bb=1-aa*cc
make/O/N=(lengthofwave) tempwave
tempwave=($wavechangex)^nn
$wavechange=$wavechange/(aa*tempwave+bb)
killwaves tempwave
Print "Delta I :", Io-Ie, "   Number of photons :", nn
print "a: ", aa, "   b: ", bb
end
macro Back()
string wavechange
wavechange=CsrWave(A)
$wavechange=backupwave
killwaves backupwave
print "You cancel the last calibration"
end#pragma rtGlobals=1          // Use modern global access method.
#pragma rtGlobals=1          // Use modern global access method.
menu "Macros"
submenu "ECalibration"
    "ECalibration"          //To calibrate the spectrum according to power changing during one
scanning.
    "CancelECali"          //To cancel the last Ecalibration.
    "ChangeScale"          //Using one standard power to unify all spectra, eg. power and photons.
end
submenu "Calibrate"
    "Calibrate"          //To connect the ending of the spectrum to the beginning of next spectrum
for two different scannings.
    "Back"          //To cancel the last calibration.
end
end
//you need to use "A cursor" to get the wave name which you want to calibrate!!
macro ECalibration(power_start, power_end,nn)
Variable power_start
Prompt power_start, "Power in the beginning :"
Variable power_end
Prompt power_end, "Power in the end :"
variable nn
prompt nn, "Number of photons :"
string wavey
string wavex
wavey=CsrWave(A)
wavex=CsrXWave(A)
variable lengthofwave

```

```

lengthofwave=numpts($wavex)
variable kslope
variable valueb
kslope=(power_end-power_start)/($wavex[lengthofwave]-$wavex[0])
valueb=power_start-kslope*$wavex[0]
make/O/N=(lengthofwave) powerline
powerline=valueb+kslope*$wavex
powerline=(1/(powerline^nn))*(power_start^nn)
$wavey=$wavey*powerline
print "-----"
print "Power at start :",power_start,"mW"
print "Power at end :",power_end,"mW"
print "Numbers of photons:", nn
print "Calibrated wave name is :", wavey
print "-----"
end
macro CancelECali()
doalert 1,"Are you sure you cancel last calibration?"
if (V_flag==1)
string wavey
wavey=CsrWave(A)
$wavey=$wavey/powerline
killwaves powerline
print "You cancel the last energy calibration"
endif
end
macro ChangeScale(power0)
variable power0
string wavechange
variable apositionvalue
variable bpositionvalue
apositionvalue=vcsr(A) //you need to use "A cursor" to get the wave name and
determinate Ie value!!
bpositionvalue=vcsr(B) // and use cursor B to determinate the value of Io.
wavechange=CsrWave(A)
//$wavechange=bpositionvalue-apositionvalue+$wavechange
//print "B:", apositionvalue,"A:", bpositionvalue
//print "Calibrated wave name is :", wavechange
//print wavechange,"+=", apositionvalue,"-", bpositionvalue,""
//$wavechange=$wavechange*(bpositionvalue/apositionvalue)
//print "B:", apositionvalue,"A:", bpositionvalue
$wavechange=((9/power0)^2)*$wavechange // Here you can set the value of the
standard power and the number of photons.
//print "Calibrated wave name is :", wavechange
//print wavechange,"*=", bpositionvalue,"/", apositionvalue
print wavechange, "*(9/", power0, ")^2"
end
macro Calibrate()
string wavechange
string wavechangex
variable Io
variable Ie
Ie=vcsr(A)
Io=vcsr(B)
wavechange=CsrWave(A)

```

```

wavechangex=CsrXWave(A)
variable lengthofwave
lengthofwave=numpts($wavechangex)
make/O/N=(lengthofwave) backupwave
backupwave=$wavechange
variable aa
variable bb
variable nn
variable cc
nn=2 //set the number of photons
cc=($wavechangex[0])^nn
aa=((Ie/Io-1)/(abs((hcsr(A))^nn-cc)))
bb=1-aa*cc
make/O/N=(lengthofwave) tempwave
tempwave=($wavechangex)^nn
$wavechange=$wavechange/(aa*tempwave+bb)
killwaves tempwave
Print "Delta I :", Io-Ie, "   Number of photons :", nn
print "a: ", aa, "   b: ", bb
end
macro Back()
string wavechange
wavechange=CsrWave(A)
$wavechange=backupwave
killwaves backupwave
print "You cancel the last calibration"
end

```

Vibrational peak fitting

Variables for equaiton 3.3 must be in a target table for these calculations.

```

n1=CC[6]+CC[7]*K[1]^2-CC[8]*K[1]^4
n2O=(CC[3]*Nu*(Nu+1)-CC[3]*K[1]^2-CC[4]*Nu^2*(Nu+1)^2-CC[5]*Nu*(Nu+1)*K[1]^2)
n2P=(CC[3]*Nu*(Nu+1)-CC[3]*K[1]^2-CC[4]*Nu^2*(Nu+1)^2-CC[5]*Nu*(Nu+1)*K[1]^2)
n2Q=(CC[3]*Nu*(Nu+1)-CC[3]*K[1]^2-CC[4]*Nu^2*(Nu+1)^2-CC[5]*Nu*(Nu+1)*K[1]^2)
n2R=(CC[3]*Nu[1+x]*(Nu[1+x]+1)-CC[3]*K[1]^2-CC[4]*Nu[1+x]^2*(Nu[1+x]+1)^2-
CC[5]*Nu[1+x]*(Nu[1+x]+1)*K[1]^2)
n2S=(CC[3]*Nu[2+x]*(Nu[2+x]+1)-CC[3]*K[1]^2-CC[4]*Nu[2+x]^2*(Nu[2+x]+1)^2-
CC[5]*Nu[2+x]*(Nu[2+x]+1)*K[1]^2)
n3O=(CC[0]*NI[x+2]*(NI[x+2]+1)-CC[0]*K[1]^2-CC[1]*NI[x+2]^2*(NI[x+2]+1)^2-
CC[2]*NI[x+2]*(NI[x+2]+1)*K[1]^2)
n3P=(CC[0]*NI[x+1]*(NI[x+1]+1)-CC[0]*K[1]^2-CC[1]*NI[x+1]^2*(NI[x+1]+1)^2-
CC[2]*NI[x+1]*(NI[x+1]+1)*K[1]^2)
n3Q=(CC[0]*NI*(NI+1)-CC[0]*K[1]^2-CC[1]*NI^2*(NI+1)^2-CC[2]*NI*(NI+1)*K[1]^2)
n3R=(CC[0]*NI*(NI+1)-CC[0]*K[1]^2-CC[1]*NI^2*(NI+1)^2-CC[2]*NI*(NI+1)*K[1]^2)
n3S=(CC[0]*NI*(NI+1)-CC[0]*K[1]^2-CC[1]*NI^2*(NI+1)^2-CC[2]*NI*(NI+1)*K[1]^2)
nO=n1+n2O-n3O
nP=n1+n2P-n3P
nQ=n1+n2Q-n3Q
nR=n1+n2R-n3R
nS=n1+n2S-n3S

```